Cellulose (2015) 22:1091–1102
DOI 10.1007/s10570-015-0563-9

ORIGINAL PAPER

Self-assembled optically transparent cellulose nanofibril films: effect of nanofibril morphology and drying procedure

Yan Qing · Ronald Sabo · Yiqiang Wu · J. Y. Zhu · Zhiyong Cai

Received: 23 September 2014 / Accepted: 26 January 2015 / Published online: 4 February 2015

Abstract Cellulose nanofibril (CNF) films currently provide great opportunity in many applications with advantages of excellent mechanical strength, high light transmittance, and good barrier properties. However, processes for preparing CNFs are typically tedious and vary, along with their properties. Here, five preparation methods using various combinations of filtration, freeze-drying, and casting are applied to produce CNF films, and their major properties are compared. Three different types of CNFs having a range of fiber diameter and aspect ratio were examined using each of these five preparation methods. Because of limited hydrogen bonds and nanofibril arrangement, the freeze-dried CNF films displayed reduced mechanical strength and light transmittance compared to the other methods, although freeze-drying was relatively fast. Some effects of film production methods on measured crystallinity were also observed with freeze-dried samples having lower crystallinity than films similarly produced by filtration and drying. Free-standing CNF films produced by casting at room temperature required long times and mold growth was sometimes observed, but cast films made from 2,2,6,6-tetramethylpiperidine-1-oxyl radical-oxidized CNFs had the highest light transmittance of any samples. Filtration of CNF suspensions followed by air- or oven-drying produced films with minimal defects, high mechanical strength, and good light transmittance with relatively little effort. Therefore, this filtration procedure is recommended for producing CNF films.

Keywords Cellulose nanofibrils · Self-assembled films · Filtration · Freeze-drying · Casting · Mechanical and optical properties

Y. Qing · Y. Wu
School of Materials Science and Engineering, Central South University of Forestry and Technology, 498 Shaoshan South Road, Changsha 410004, China

Y. Qing · R. Sabo (✉) · J. Y. Zhu · Z. Cai (✉)
Forest Products Laboratory, United States Department of Agriculture, 1 Gifford Pinchot Drive, Madison, WI 53726-2398, USA
e-mail: rsabo@fs.fed.us

Z. Cai
e-mail: zcai@fs.fed.us

Introduction

Because it has become increasingly desirable to develop materials from sustainable resources, lignocellulosics and cellulose nanomaterials in particular have recently received a great deal of attention for their potential to replace materials created from nonsustainable resources. Among the promising characteristics of cellulosic nanomaterials is their high strength, with the crystalline region of cellulose having an elastic modulus of about 150 GPa (Cheng and Wang 2008; Iwamoto et al. 2009). Cellulose nanofibrils (CNFs),

one type of cellulose nanomaterial, were first reported in the early 1980s (Herrick et al. 1983; Turbak et al. 1983). CNFs are typically isolated using high-intensity mechanical fibrillation of coarse lignocellulosic fibers typically in combination with chemical or enzymatic pretreatment (Pääkkö et al. 2007; Saito et al. 2009; Qing et al. 2013b). CNFs are typically entangled networks of nanoscale cellulose fibrils, having high aspect ratio and a large specific surface area, and they have been shown to have interesting and useful properties. For example, CNF nanofibrils uniformly dispersed in the aqueous suspension present as stable gels even at solids concentrations as low as 0.3 % (Pääkkö et al. 2007), and films formed from CNFs have been reported as having low coefficients of thermal expansion, good mechanical strength, and high transparency. Therefore, many attempts have been devoted to develop green and high-quality CNF products with applications including barrier and transparent films, engineering polymeric composites, and functional aerogels (Capadona et al. 2007; Okahisa et al. 2009; Aulin et al. 2010; Olsson et al. 2010).

Films made from CNFs are of particular interest because of their properties and because of their analogy to papermaking in which the fiber suspensions can be dewatered and formed into sheets. When removing the water (or other solvent) from a CNF suspension, the adjacent individual nanofibrils initially collapse by the capillary force and later form strong hydrogen bonds between hydroxyl groups, which are abundant on the fiber surface (Nyström et al. 2010). The obtained films are dense, stiff, and transparent and exhibit layered and possibly even porous structures, depending on the properties of the raw nanofibrils and the dewatering process. The tensile strength and elastic modulus for the films reported in the literature ranged from 100–230 MPa to 8–15 GPa, respectively, and varied depending on fiber resources and processing conditions. Notably, orientated 2,2,6,6-tetramethylpiperidine-1-oxyl radical- (TEMPO-)oxidized CNF films with the degree of fiber orientation more than 80 % showed tensile strength and modulus as high as 400 MPa and 33 GPa, respectively (Sehaqui et al. 2012). Because of extremely small diameters (usually much less than 100 nm) of CNFs, the scattering and absorption of visible light by the nanofibrils is limited, which leads to highly transparent CNF films. A 20-μm-thick TEMPO-oxidized CNF film prepared with fiber diameters of 3–4 nm is reported to achieve 90 % transmittance at the wavelength of 600 nm (Fukuzumi et al. 2009). Nanofibrils are randomly deposited into layered structures with small pores that are not interconnected, resulting in films with porosities on the order of 10 %. Thus, low molecular weight substances like oxygen, carbon oxidation, and oil are limited to permeate through the networked films (Fukuzumi et al. 2009; Aulin et al. 2010; Qing et al. 2013a, b). The good barrier performance makes it possible to be regarded as a potential substitution for conventional fossil-derived plastic products in package and carrier. Since then, the widely demonstrated applications for CNF films range from coating, package, medical carrier, to loudspeaker membranes, transparent LED substrate, battery electrodes, and flexible electronics (Henriksson and Berglund 2007; Okahisa et al. 2009; Aulin et al. 2010; Nyström et al. 2010; Sabo et al. 2012).

Two predominant approaches are reported in the literature for preparing CNF films. One popular method is solution casting, by which nanofibril suspensions are kept in open containers, and the solvent, usually water, is allowed to gradually evaporate (Aulin et al. 2010). Casting is a time-consuming process, typically taking days or weeks. For example, Sehaqui et al. (2010) reported that preparing 40-μm-thick films with a diameter of 80 mm under atmospheric conditions starting with CNF concentration of 0.2 wt% took more than 120 h. To accelerate the processing, the castings are sometimes carried out with slight heating under vacuum (Spence et al. 2010; Xhanari et al. 2011; Rodionova et al. 2012). A second popular and relatively fast method to produce CNF films involves the filtration of CNF solutions and drying the obtained hydrogels (Henriksson et al. 2008; Qing et al. 2013b). In this method, which is similar to a paper-making process, CNF suspensions are filtered under vacuum or pressure using membranes with pores typically hundreds of nanometers in diameter (Fukuzumi et al. 2009; Sehaqui et al. 2010; Qing et al. 2013b). Various methods have been used to dry the resulting hydrogels including air-drying (Qing et al. 2013b), oven drying (Henriksson et al. 2008; Fukuzumi et al. 2009), and hot-pressing (Nakagaito and Yano 2005). Sehaqui et al. (2010) even reported a processing technique in which a CNF gel "cake" was vacuum- and hot-dried in a special apparatus resulting in a drying time of about 1 h. Freeze-drying, which allows aqueous solvents in the suspension to directly sublimate

from a solid to gas phase of dilute CNF suspensions, is a popular method to prepare CNF aerogels having high porosity (Pääkkö et al. 2008; Svagan et al. 2010). In the current work, freeze-drying is explored as an alternative route for drying the wet CNF hydrogels. Freeze-drying reduces the collapse between neighboring nanofibrils and largely limits shrinkage, especially wrinkling at the edge of CNF films. The properties of films from these different methods vary significantly, although the contribution of the processing conditions on these property variations is not clear.

Variations in microstructure of CNFs and their films are known to significantly impact the performance of the films. For example, Henriksson et al. (2008) reported that mechanical strength of CNF films was strongly dependent on the degree of polymerization (DP) of raw nanofibrils and on the porosity of films. Similarly, Retegi et al. (2010) prepared bacterial cellulose (another kind of cellulose nanofiber) films with controlled density by varying compression pressures. They found that the tensile modulus was linearly enhanced with increasing mold pressure, which also led to slight increases in tensile strength. CNF film preparation procedures affect the films' shrinkage, appearance, strength, vapor permeability, and opacity (Dalmas et al. 2007; Retegi et al. 2010; Sehaqui et al. 2010). However, the effect of preparation methods on the final properties of CNF films has not been studied in detail.

Therefore, in the current work we prepared CNF films using various processing conditions, namely casting and filtration followed by either air- or freeze-drying. In addition, the effect of hot-pressing on the properties of CNF films was examined to produce flat, wrinkle-free films. Three kinds of cellulose nanofibrils having different morphologies were used to create films using multiple processing techniques to further elucidate the roles of raw materials and processing on the physical and mechanical properties of the films. The appearance, morphology, porosity, mechanical properties, and visible light transmittance of the obtained films were characterized and are reported here.

Materials and methods

Preparation of CNFs

Three kinds of cellulose nanofibrils were used in this study to prepare CNF films; they are TEMPO-oxidized nanofibrils, nanofibrils refined with multiple enzyme pretreatments (MER) and the MER nanofibrils followed by microfluidization (MERM). The starting cellulose fibers were fully bleached kraft eucalyptus. Detailed descriptions of the preparation procedures were previously reported by Qing et al. (2013a, b) and are briefly described here. TEMPO-oxidized CNFs were produced according to the method reported by Saito et al. (2009). Enzyme-treated CNFs (MER and MERM) were prepared by pretreating the pulp fiber suspensions at a solid consistency of 1.5 % with commercial enzymes with trade names FiberCare® Cellulclast 1.5 L from Novozymes (Franklinton, NC, USA). The enzyme pretreated fibers were then mechanically refined for 6 h using a MKZA6-2 SuperMass-Colloider (Masuko Sangyo Co., Ltd., Saitama, Japan) at 15,000 rmp with a disk gap of −5 μm, and these samples were labeled as MER. A portion of the obtained MER nanofibrils were subjected to further intense fibrillation in a M-110EH-30 Microfluidizer (Microfluidics, Newton, MA, USA). The fiber suspension was diluted to 1 % solids and passed through an 87-μm chamber 15 times at pressure of 138 MPa, and these samples were labeled as MERM.

Preparation of CNF films

CNF films were prepared by either solution casting or by filtering CNF suspensions followed by air-, oven- or freeze-drying the wet hydrogel films. In some cases, the films were also hot-pressed. Altogether, five different processing methods were examined, and these processing methods are illustrated in Fig. 1.

Four of the five methods involved first filtering CNF suspensions to obtain a hydrogel film, which could then be further dried using various conditions. The filtration procedure was performed by first diluting the CNF

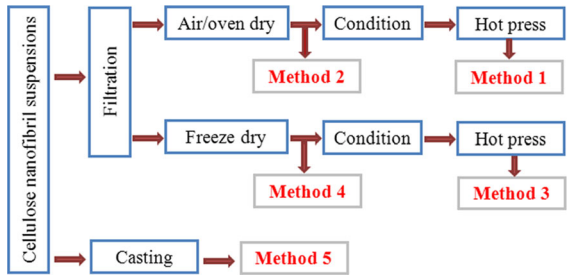

Fig. 1 Various processing methods for preparation of self-assembled CNF films

suspensions to 0.2 % solids by weight with reverse-osmosis-treated (RO) water, then filtering the suspensions using a 142-mm Millipore ultrafiltration system (Millipore Corporation, Billerica, MA, USA) under 0.55 MPa of air pressure. Omnipore^{TM} filter membranes with pore size of 0.1 μm (JVWP14225, JV, Millipore Corporation, USA) were supported on filter paper in the ultrafiltration system. The wet films (hydrogels) were peeled from the membrane and processed by one of the four methods. In methods 1 and 2, the hydrogels were stacked and placed between an assembly of waxy coated papers, absorbent blotter paper, and two metal caul plates air-dried at room temperature for 24 h and then oven-dried at 60 °C for 8 h under a load of approximately 250 N. The blotter and filter papers were replaced several times over the first 24 h to minimize wrinkling of the films. This process was denoted as "method 2." In method 1, samples that were prepared as described in method 2 were subsequently conditioned at 65 % relative humidity and 23 °C for 5 days then hot-pressed at 105 °C for 3 min with pressure of 0.6 MPa. Methods 3 and 4 both involved freeze-drying the hydrogels by first freezing them at −18 °C for 12 h and then freeze-drying them under a vacuum of 0.01 MPa with a cooling coil temperature of −60 °C for 8 h using a Labconco freeze-drying system (Kansas City, MO, USA). The process ending with the freeze-drying was denoted as "method 4." As with the air- or oven-drying method, some of the freeze-dried samples were conditioned at 65 % relative humidity and 23 °C for 5 days followed by hot-pressing at 105 °C for 3 min with pressure of 0.6 MPa; this process was denoted as "method 3." Finally, "method 5" involved the solution casting of CNF suspensions diluted to 0.5 % solids concentration with RO water. The diluted suspensions were first degassed under a vacuum of 0.0275 MPa for 1 h then carefully poured onto polystyrene petri dishes having diameter of 132 mm. The solutions were statically maintained at room temperature until the free-standing films were separated from the polymer plates themselves.

Characterization of CNF and CNF films

Morphological characterization of CNF nanofibrils

The morphology of different cellulose nanofibrils was observed by transmission electron microscopy (TEM). For preparation of TEM samples, diluted CNF suspension were deposited to the glow-discharged copper grid with formvar and carbon film (400 mesh). The droplet was maintained on the grid for 2 min, and then rinsed thoroughly using a 2 % aqueous uranyl acetate stain followed by blotting dry. Samples were imaged using Philips CM-100 TEM (Philips/FEI Corporation, Eindhoven, Holland) operated at 100 kv, spot 3,200-μm condenser aperture, and 70-μm objective aperture. The images were captured using a SIA L3C 4-2M pixel CCD camera (Scientific Instruments and Application, Duluth, GA, USA) with 46 k magnification. The diameter of different CNFs was measured and calculated from TEM images using the GNU Image Manipulation Program (GIMP, free download from http://www.gimp.org/) software. A minimum of 50 measurements were made to evaluate the fiber diameter for at least five images for each type of CNF.

Microstructure of CNF films

X-ray diffraction (XRD) patterns for different CNF films were obtained with a Bruker/Siemens Hi-Star 2d diffractometer (Bruker AXS, Madison, WI, USA) using CuKa radiation generated at 40 kV and 30 mA. The dried homogenous CNF films were individually mounted in a special holder through which an X-ray beam centrally passed. Scattering radiation was detected in a 2θ range from 2° to 40° at scanning rate of 4°/min. The crystallinity index (CI) was calculated from the XRD patterns following the equation $CI = [(I_{200} - I_{am})/I_{200}] \times 100\ \%$, with accordance of the Segal method (Segal et al. 1962; Cheng et al. 2007). I_{200} is the intensity height of crystalline (200) peak (at $2\theta = 22.5°$), and I_{am}, which represents the intensity from the amorphous region, is the minimum value of the intensity near $2\theta = 18°$.

Tensile test for CNF films

The tensile properties of CNF films were tested using an Instron 5865 universal material testing apparatus (Instron Engineering Corporation, Norwood, MA, USA) with a 500-N load cell, according to ASTM D638-10. The specimens were cut to conform to ASTM D638-10 type V dogbone shape using a special die (Qualitest, Ft. Lauderdale, FL, USA) and conditioned at 50 % RH and 23 °C for 1 week. The tests

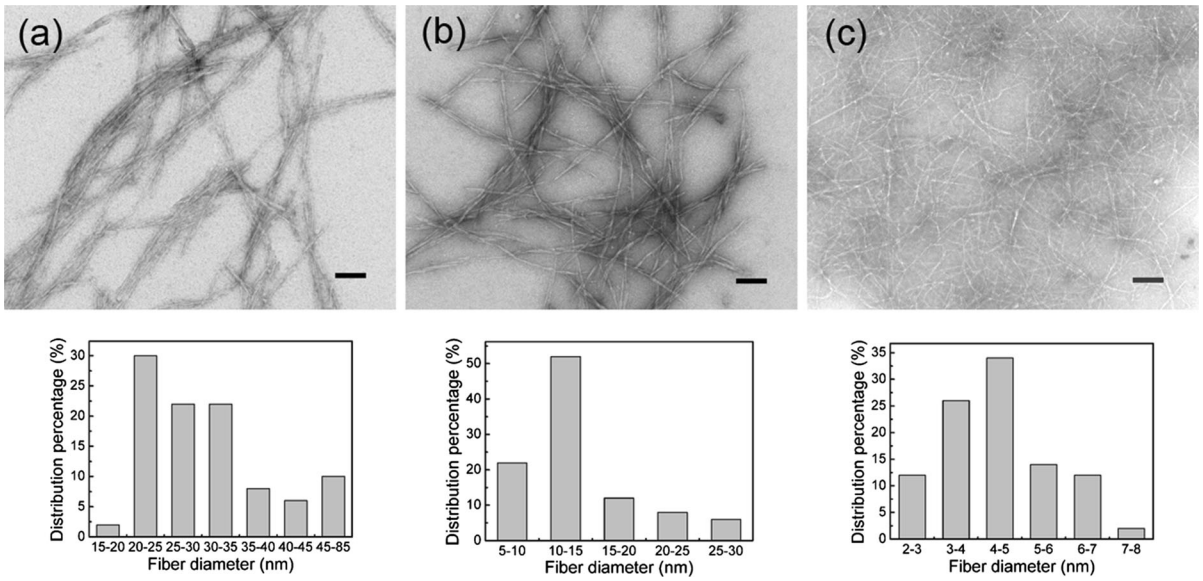

Fig. 2 TEM images (*up*) and size distributions (*below*) of different CNFs. **a** MER; **b** MERM; and **c** TEMPO. The *scale bars* are 100 nm

were conducted at a cross-head speed of 1 mm/min in a room conditioned at 50 % RH and 23 °C, and a pre-load of 5 N was applied to remove slack. At least six specimens were tested for each condition. An LX 500 laser extensometer (MTS Systems Corporation, Eden Prairie, MN, USA) was used to determine the displacement with sampling frequency of 10 Hz. The laser recorded the displacement between two strips of reflective tape initially placed approximately 8 mm apart on the necked-down region of the dog-bone specimens. Strain was calculated from the determined extension and initial gauge length. Film density was calculated gravimetrically by measuring the dimension and weight of well-defined sections of each film. The corresponding porosity was estimated by the following equation:

$$\text{Porosity} = \left(1 - \frac{\rho_{\text{fil}}}{\rho_{\text{cel}}}\right) \times 100\,\%$$

Here ρ_{fil} and ρ_{cell} are the densities of the obtained CNF film and neat cellulose (1,500 kg/m^3), respectively.

UV–Vis light transmittance

The visible light transmittance for CNF films was measured at a wavelength range from 400 to 800 nm using an U-4100 ultraviolet–visible (UV–Vis) spectrometer (Hitachi High Technologies America Inc., Schaumburg, IL, USA). Rectangular specimens with size of 40 mm × 9 mm (length × width) were placed in a quartz cuvette and measured by placing it 25 cm away from the entrance port of the integrating sphere. The specimens were conditioned at 50 % RH and 23 °C for 2 days prior to testing, and two tests were performed for each sample.

Results and discussion

Morphological characteristic of nanofibrils

Transmission electron micrographs of the CNFs (Fig. 2) reveal that all the nanofibrils are of fine widths less than 100 nm. The diameters of the CNFs were evaluated from the TEM images, and their distributions are shown in Fig. 2. The network structure of the interconnected nanofibrils makes it extremely difficult to detect the length of individual fibrils from the images, so these are not reported here.

For the most part, the three types of CNFs are networked, although MERM CNFs appear to be less networked and contain some discreet rod-shaped particles. The TEMPO-oxidized CNFs have uniform diameters in the range of 3–8 nm, are highly networked, and have high aspect ratios (fiber length/diameter). The chemical oxidation reaction to produce

these fibers creates repulsive forces that contribute to the separation of individual microfibrils (Saito et al. 2009). This chemo-mechanical fibrillation also primarily conserves the original cellulose structure further resulting in good physical and mechanical properties (Siró and Plackett 2010). The enzymatically and mechanically treated MER and MERM CNFs appear wider and shorter than the TEMPO CNFs. The MER CNFs have a significant number of fiber bundles with diameters ranging from about 15 to 85 nm. Further refining in a Microfluidizer resulted in decreased diameters (5–30 nm) and a reduction in the number of fibril aggregates. Similar results were shown in our previous work (Qing et al. 2013a, b), in which extensive enzymatic and mechanical treatments resulted in CNFs containing predominantly discreet rod-shaped particles. However, in the current work, MERM appears somewhat more networked than the fibers undergoing treatment similar to that in the previous report. Nonetheless, the Microfluidizer clear results in CNFs with reduced diameters and breaks apart some of the network structure.

Film appearance and preparation time

Photographs of CNF films prepared by the different processing conditions are shown in Fig. 3. The freeze-dried films are clearly more opaque than the cast or pressed films. The freeze-dried films created from enzymatic and mechanical treatments are completely opaque and appear white, whereas the freeze-dried TEMPO CNF films are translucent with some spots more opaque than others. Freeze-drying reduces the capillary forces responsible for collapsing fibers, thus preventing them from hydrogen bonding as they would when cast or dried under pressure (Pääkkö et al. 2008; Peng et al. 2012). Therefore, microgaps generated among interconnected nanofibrils significantly increase the light scattering because of the difference in refractive index between the nanofibrils (1.54) and air (1.0) (Mark 2007). This limitation of capillary force collapse during freeze-drying subsequently conserves the initial state of loose nanofibrils. Okamoto and Meshisuka (2010) showed that wood pulp fiber dried by freeze-drying (or supercritical drying) were more swollen than when dried by conventional air-drying.

Significant moisture gradients are created between the surface and core of the films during drying, especially in the freeze-drying and casting process. This moisture gradient creates residual stresses, which result in deformation of the films, which can be clearly seen as rough films for methods 4 and 5 in Fig. 3. Further conditioning, which allows for moisture absorption and subsequent hot-pressing, resulted in much smoother surfaces for the freeze-dried films (as shown for method 3 in Fig. 3). On the other hand, the constrained drying between absorbent papers (method 2) resulted in smooth surfaces without further conditioning and hot-pressing. Interestingly, the cast MERM CNF films shrank significantly compared to all other types of CNFs and process conditions. This happened for each of the three replicates, and the phenomena is not readily understood. During the casting process, the center of the drying films was observed to become solid-like before the outer regions. Perhaps the smaller, more discreet CNFs in the MERM samples were more likely to move and displace water than the more networked CNFs in the other samples. However, further investigation of this phenomenon is warranted as it may have implications in processing and properties of materials containing these types of CNFs. Another observation worthy of note is that cast CNF films sometimes developed mold growth. Overall, films prepared by methods 1 and 2 appear to have the most consistent and desirable appearance.

Efficient preparation of CNF films is one concerning issue for industrial scalability as dewatering and drying require a great deal of time and energy. The preparation times for producing CNF films in this study varied from about 30 h to more than 2 weeks. Solution casting took the longest amount of time with films of about 100-μm thicknesses taking at least 2 weeks to dry under ambient conditions. The filtration process for TEMPO CNFs was slower than for the enzymatically treated CNFs, but all samples reported here were left in the filtration apparatus for 10 h. The process could be sped up dramatically by using filtration membranes with larger pores in a method similar to that reported by Sehaqui et al. (2010), in which pore sizes of about 650 nm were used instead of the 100-nm pore sizes used in this study. Rapid drying of the films is possible, such as in a hot press at elevated temperatures. However, rapid drying often results in deformation or blow-out of the sheet resulting in holes or sheets with undesirable appearance. Sehaqui et al. (2010) also reported that films

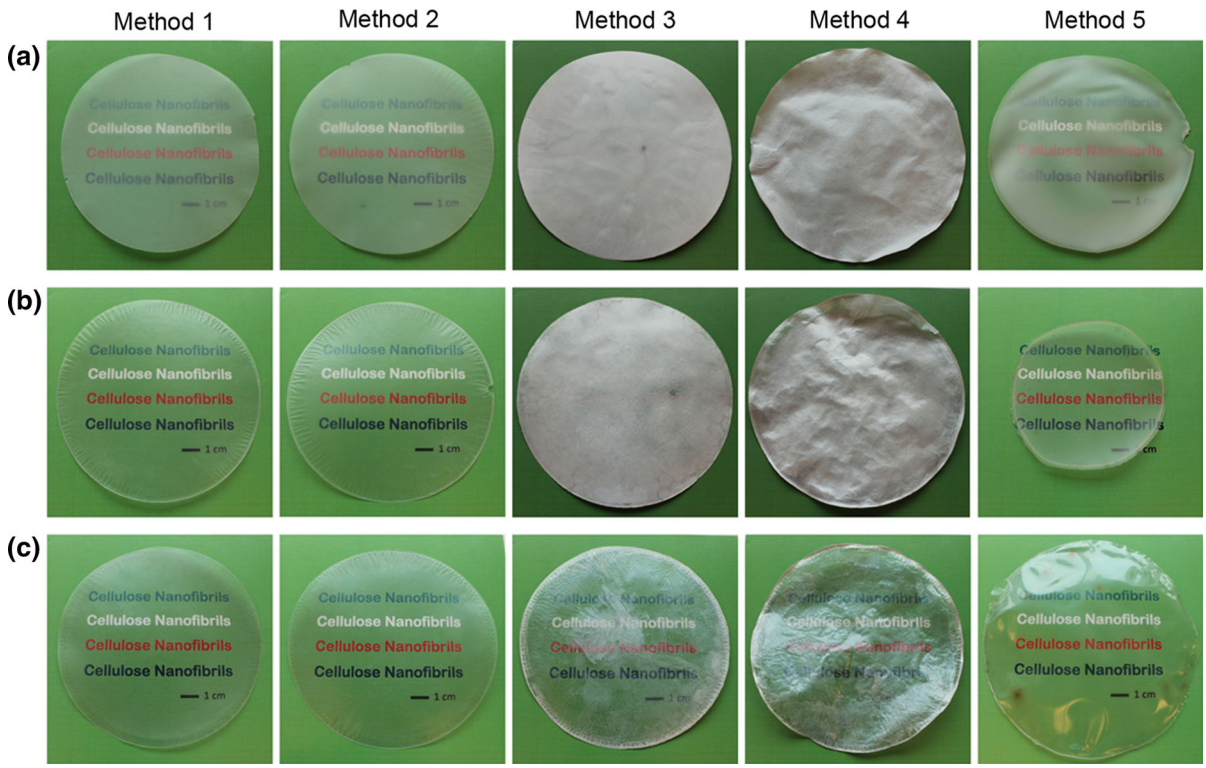

Fig. 3 Photographs of different CNF films. The *scale bar* in the background is 1 cm and dimension of *green squares* are 122 (length) × 124 (height) mm. **a** MER; **b** MERM; and **c** TEMPO

dried rapidly in a hot press had slightly lower mechanical properties than those dried slowly. Freeze-drying was relatively fast with frozen sheets taking only about 8 h to become dry. Because slow drying is easy, reproducible, and produces smooth films with good mechanical and optical properties, it is the preferred method, although more rapid methods are certainly available.

Light transmittance

The use of transparent films and composites is of interest in many applications, so the light transmittance of various CNF films is compared in Fig. 4. Because of the extremely fine nanofibril diameter, CNF films are typically fairly transparent over the visible light range. The data show that films made from smaller diameter nanofibrils have higher light transmittance, so TEMPO CNF films transmit more light than MERM CNF films, which in turn transmit more light than MER CNF films. Cast TEMPO CNF films showed the greatest light transmittance of any other method or (type of CNF films) likely because cast films are known to have low surface roughness and thus scatter less light (Nogi et al. 2009). Similar results were reported by Sehaqui et al. (2010), who found that cast CNF films were smoother using atomic force microscopy (AFM). TEMPO CNF films made from methods 1 and 2 have the second highest light transmittance of the samples. Even freeze-dried TEMPO CNF films were fairly translucent with the exception of some spots as discussed previously. However, freeze-dried MERM and MER CNF films were translucent, and no light transmittance was measured for them. Interestingly, the films cast from MERM and MER CNFs had lower light transmittance than corresponding films made from methods 1 and 2. This reduced transparency is readily explained for MERM and MER films, which shrank and thus were thicker when cast than when pressed. According to the Beer–Lambert Law, the absorption of light is exponentially reduced with the thickness, and this is roughly the case with the current data. The thickness of MERM-cast films was about 80 % greater

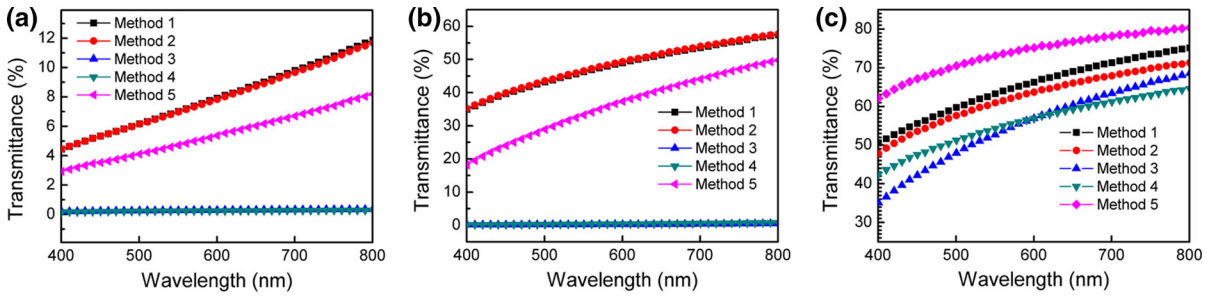

Fig. 4 Visible light transmittance of different CNF films. **a** MER; **b** MERM; **c** TEMPO

(160 μm) than those made using method 1 (90 μm), and the thickness of MER cast films was about 10 % greater (100 μm) than those made using method 1 (90 μm). Therefore, even though cast MERM and MER films appeared smoother than some of the others (Fig. 3), they had lower light transmittance, primarily because of their increased thickness compared to films dried under constraint. Obviously, both the nanofibril and film processing procedures have a significant impact on the optical properties of CNF films.

CNF film structure

Because the microstructures of cellulose nanomaterials have significant influence on their mechanical properties (Uddin et al. 2011; Sehaqui et al. 2012), the films in this study were examined using a 2-D XRD diffractometer. Ring patterns (not shown here) perpendicular to the film plane showed no preferential alignment of the cellulose crystals, suggesting that the nanofibrils were randomly oriented. This random orientation is in agreement with other studies showing CNFs are irregularly connected and form random in-plane orientation upon drying (Henriksson et al. 2008; Sehaqui et al. 2012).

The XRD patterns and calculated crystallinity for the films are shown in Fig. 5. The strong and sharp diffraction peak at $2\theta = 22.3°$ corresponds to the (200) lattice plane of cellulose I (Tonoli et al. 2012), which is characteristic of natural plant cellulose. For all three types of CNFs, the measured crystallinity index (CI) was higher for films, which were hot-pressed, especially for freeze-dried films. Previous studies (Kummar and Kothari 1999; Retegi et al. 2010; Qing et al. 2013a, b) found similar results, and those authors concluded the compression led to reorientation of the fibrils. Heat and moisture has also been

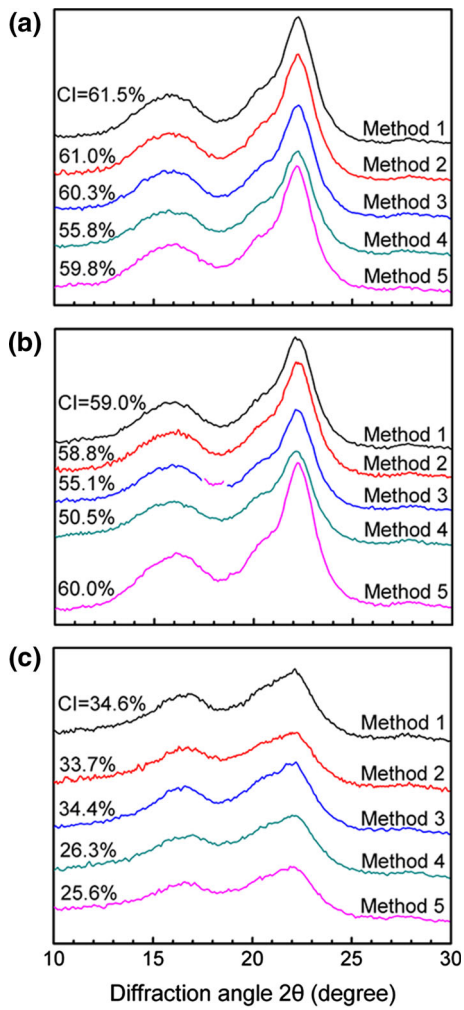

Fig. 5 Typical XRD patterns for various CNF films. **a** MER; **b** MERM; **c** TEMPO

reported to increase the cellulose crystallinity of wood and pure cellulose (Bhuiyan et al. 2000). Therefore, the increase in measured crystallinity is believed to be

real and not simply an artifact of the measurement technique.

In addition, measured density and calculated porosity values for the various CNF films are shown in Fig. 6. Although some trends are apparent, the density measurements had relatively high variability, so many of the values are statistically similar. For example, freeze-dried films often, but not always, had lower densities than filtered and hot-pressed films. Freeze-dried MER and MERM CNF films from methods 3 and 4 both had significantly lower densities than their respective films filtered and hot-pressed (method 1) or cast (method 5). However, freeze-dried and hot-pressed TEMPO CNF films (method 3) had statistically lower density than filtered and hot-pressed (method 1) TEMPO CNF films. The densities of all other TEMPO CNF films were statistically similar. In this work, the densities were measured gravimetrically by measuring the weight and dimensions of the samples. The thickness was measured using a caliper, and freeze-dried samples seemed to deform more than other samples. Therefore, the density values reported here for freeze-dried specimens may be artificially high. Similar results were reported by Sehaqui et al. (2010), who revealed that the density of CNF films estimated gravimetrically is slightly higher than when immersing samples into mercury (Henriksson et al. 2008). Because of large variability in density measurements, the effect of hot-pressing on air- or oven-dried CNF films was not seen to be statistically significant. However, note that in many cases only the hot-pressed CNF films (method 1) were revealed to be statistically denser than freeze-dried films. Perhaps a more accurate method for evaluating density would reveal that hot-pressing increases the density of filtered and dried films as reported by Retegi et al. (2010). Finally, MER CNF films generally had significantly lower density values than MERM or TEMPO CNF films. This is likely due to the larger size of the MER CNFs, which would likely not pack as well and have less surface area for bonding.

Mechanical properties

Differences in the tensile strength of the various CNF films were observed as shown in Fig. 7. Clearly, films prepared from TEMPO-oxidized nanofibrils have superior strength to the films prepared from enzymatically treated nanofibrils. The tensile stress at break of the TEMPO CNF films was in the range of 175–225 MPa, whereas the tensile stress at break for MER and MERM CNF films was in the range of 60–120 MPa. However, no difference in tensile strength between MER and MERM CNFs was observed. These results are similar to previously reported results (Qing et al. 2013a, b) and are likely a result of the morphology of the nanofibrils, which is known to significantly impact the mechanical properties of CNF films (Henriksson et al. 2008). TEMPO CNFs formed strong nanofibril hydrogen bonds because of sufficient carboxyl groups, uniform diameters, high aspect ratio, and significant entanglement,

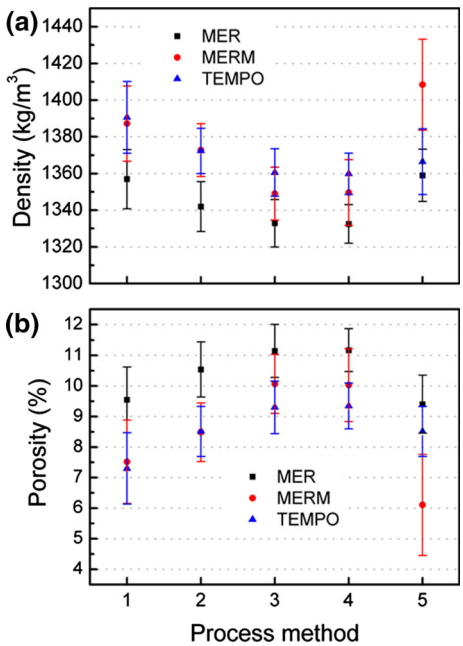

Fig. 6 Density (**a**) and porosity (**b**) of different CNF films

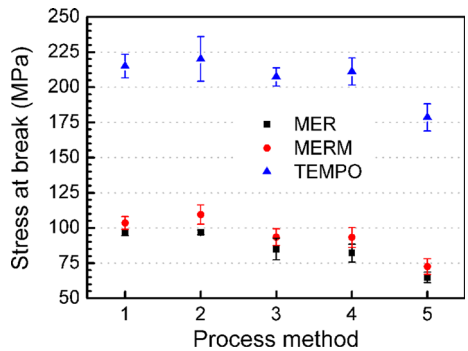

Fig. 7 Tensile strength of CNF films

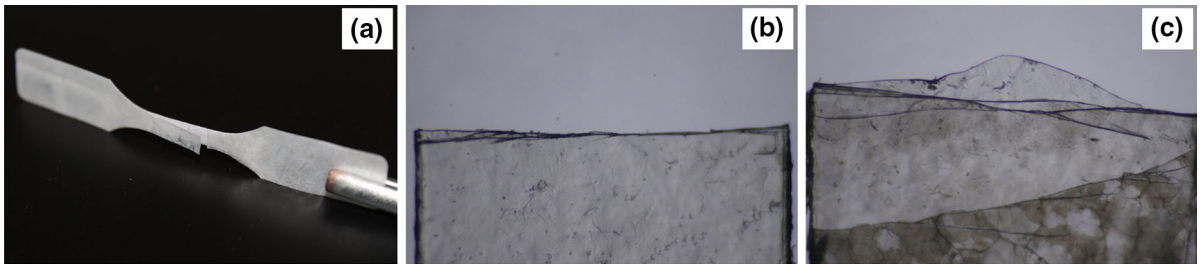

Fig. 8 Optical images of tensile tested CNF films that were freeze-dried using method 4 (**a** and **c**) and oven dried using method 2 (**b**)

resulting mostly in films with good mechanical properties (Saito et al. 2009; Qing et al. 2013a, b).

The processing method for producing the CNF films also significantly affected the tensile strength of the films. Cast films for all three types of CNF films had lower strength than the other methods of producing films from the same type of nanofibrils. The reason that cast films had lower tensile strength is not clear, but one explanation is that these cast films sometimes exhibited visible mold growth, which may have deteriorated the integrity of the films. The addition of biocides to these CNF suspensions would prevent mold growth, but this was not the practice for the current study. However, Sehaqui et al. (2010) also reported that cast films had slightly lower mechanical properties than films produced by filtering and oven-drying. Hot-pressing the CNF films did not significantly improve the tensile strength, unlike the results reported by Retegi et al. (2010) in which hot-pressing bacterial CNFs resulted in increased mechanical properties. However, in that case, the pressure applied was extremely high (100 MPa) compared to less than 1 MPa in the current study. MER CNF films produced by freeze-drying (methods 3 and 4) had lower tensile strength than MER CNF films produced by filtering and air- or oven-drying (methods 1 and 2), and MERM CNF films produced by freeze-drying had lower tensile strength than MERM CNF films produced by method 2. However, freeze-dried and air- or oven-dried TEMPO CNF films did not have significantly different tensile strength. One plausible explanation for the reduced tensile strength of some of the freeze-dried films is due to decreased density, although the correlation between density and tensile strength is somewhat tenuous. Another possible explanation is that freeze-dried CNFs often exhibited tensile failure as delamination instead of a clean break as shown in Fig. 8. This indicates that the interlaminar adhesion in freeze-dried films is weak, and the failure of an individual layer may result in lower mechanical strength.

Conclusions

Processing conditions for producing cellulose nanofibrils, as well as the process conditions for producing CNF films significantly impact the mechanical and physical properties of the films. TEMPO CNF films had better tensile strength and higher transparency than CNF films made from enzymatically and mechanically treated CNF films. Cast TEMPO CNF films had the highest transparency of any of the films, but cast films from enzymatically treated films had lower transparency than filtered and air- or oven-dried films made from corresponding starting CNFs. Cast films also had lower tensile strength than other films made from the same type of CNFs. Cast films took weeks to dry and sometimes exhibited mold growth, so biocides are recommended for use in CNF suspensions that will be cast. Freeze-dried films generally had lower densities than air- or oven-dried films, and for enzymatically treated CNFs, the tensile strength of freeze-dried films was lower than that of air- or oven-dried films. Freeze-dried films were also typically translucent. The attempt to remove residual stresses by conditioning CNF films at elevated humidity followed by hot-pressing did not result in significant improvements in film properties. Because slow drying is easy, reproducible, and produces smooth films with good mechanical and optical properties, it is the preferred method in our laboratory, but more rapid methods are certainly available.

Acknowledgments This work was financially supported by Agriculture and Food Research Initiative Grant (No. 2011-67009-20056) from the USDA National Institute of Food and Agriculture the Forestry, Industry Research Special Funds for Public Welfare Project of China (201404604), and Hunan Provincial Innovation Foundation for Postgraduate (CX2014A013) from China. The authors gratefully acknowledge Rick Reiner of the Forest Products Laboratory for preparing and supplying TEMPO-oxidized cellulose nanofibrils. Debby Sherman of DS Imaging is kindly acknowledged for TEM imaging.

References

Aulin C, Gällstedt M, Lindström T (2010) Oxygen and oil barrier properties of microfibrillated cellulose films and coatings. Cellulose 17(3):559–574

Bhuiyan MTR, Hirai N, Sobue N (2000) Changes of crystallinity in wood cellulose by heat treatment under dried and moist conditions. J Wood Sci 46(6):431–436

Capadona JR, Berg OVD, Capadona LA, Schroeter M, Rowan SJ, Tyler DJ, Weder C (2007) A versatile approach for the processing of polymer nanocomposites with self-assembled nanofiber templates. Nat Nanotechnol 2(12):765–769

Cheng Q, Wang S (2008) A method for testing the elastic modulus of single cellulose fibrils via atomic force microscopy. Compos A 39(12):1838–1843

Cheng Q, Wang S, Rials TG, Lee SH (2007) Physical and mechanical properties of polyvinyl alcohol and polypropylene composite materials reinforced with fibril aggregates isolated from regenerated cellulose fibers. Cellulose 14(6):593–602

Dalmas F, Cavailé JY, Gauthier C, Chazeau L, Dendievel R (2007) Viscoelastic behavior and electrical properties of flexible nanofiber filled polymer nanocomposites. Influence of processing conditions. Compos Sci Technol 67(5):829–839

Fukuzumi H, Saito T, Iwata T, Kumamoto Y, Isogai A (2009) Transparent and high gas barrier films of cellulose nanofibers prepared by TEMPO-mediated oxidation. Biomacromolecules 10(1):162–165

Henriksson M, Berglund LA (2007) Structure and properties of cellulose nanocomposite films containing melamine formaldehyde. J Appl Polym Sci 106(4):2817–2824

Henriksson M, Berglund LA, Isaksson P, Lindström T, Nishino T (2008) Cellulose nanopaper structure of high toughness. Biomacromolecules 9(6):1579–1585

Herrick FW, Casebier RL, Hamilton JK, Sandberg KR (1983) Microfibrillated cellulose: morphology and accessibility. J Appl Polym Sci Appl Polym Symp 37(9):797–813

Iwamoto S, Kai W, Isogai A, Iwata T (2009) Elastic modulus of single cellulose microfibrils from tunicate measured by atomic force microscopy. Biomacromolecules 10(9): 2571–2576

Kummar V, Kothari SH (1999) Effect of compressional force on the crystallinity of directly compressible cellulose excipients. Int J Pharm 177(2):173–182

Mark JE (ed) (2007) Physical properties of polymers handbook, 2nd edn. Springer, New York, pp 825–850

Nakagaito AN, Yano H (2005) Novel high-strength biocomposites based on micro fibrillated cellulose having nano-order-unit web-like network structure. Appl Phys A 80(1):155–159

Nogi M, Iwamoto S, Nakagaito AN, Yano H (2009) Optically transparent nanofiber paper. Adv Mater 21(16):1595–1598

Nyström G, Mihranyan A, Razaq A, Lindström T, Nyholm L, Strømme M (2010) A nanocellulose polypyrrole composite based on microfibrillated cellulose from wood. J Phys Chem B 114(12):4178–4182

Okahisa Y, Yoshida A, Miyaguchi S, Yano H (2009) Optically transparent wood-cellulose nanocomposite as a base substrate for flexible organic light-emitting diode displays. Compos Sci Technol 69(11–12):1958–1961

Okamoto T, Meshisuka G (2010) The nanostructure of kraft pulp 1: evaluation of various mild drying methods using field e scanning electron microscopy. Cellulose 17(6):1171–1182

Olsson RT, Azizi Samir MAS, Salazar-Alvarez G, Belova L, Ström V, Berglund LA, Ikkala O, Nogués J, Gedde UW (2010) Making flexible magnetic aerogels and stiff magnetic nanopaper using cellulose nanofibrils as templates. Nat Nanotechnol 5(8):584–588

Pääkkö M, Ankerfors M, Kosonen H, Nykänen A, Ahola S, Österberg M, Ruokolainen J, Laine J, Larsson PT, Ikkala O, Lindström T (2007) Enzymatic hydrolysis combined with mechanical shearing and high pressure homogenization for nanoscale cellulose fibrils and strong gels. Biomacromolecules 8(6):1934–1941

Pääkkö M, Vapaavuori J, Silvennoinen R, Kosonen H, Ankerfors M, Lindström T, Berglund LA, Ikkala O (2008) Long and entangled native cellulose I nanofibers allow flexible aerogels and hierarchically porous templates for functionalities. Soft Matter 4(12):2492–2499

Peng Y, Gardner DJ, Han Y (2012) Drying cellulose nanofibrils: in search of a suitable method. Cellulose 19(1):91–102

Qing Y, Sabo R, Wu Y, Cai Z (2013a) Resin impregnation of cellulose nanofibril films facilitated by water swelling. Cellulose 20(1):303–313

Qing Y, Sabo R, Zhu JY, Agarwal U, Cai Z, Wu Y (2013b) A comparative study of cellulose nanofibrils disintegrated via multiple processing approaches. Carbohydr Polym 97(1):226–234

Retegi A, Gabilondo N, Peña C, Zuluaga R, Castro C, Gañan P, de la Caba K, Mondragon I (2010) Bacterial cellulose films with controlled microstructure–mechanical property relationship. Cellulose 17(3):661–669

Rodionova G, Eriksen Ø, Gregersen Ø (2012) TEMPO-oxidized cellulose nanofiber films: effect of surface morphology on water resistance. Cellulose 19(4):1115–1123

Sabo R, Seo JH, Ma Z (2012) Cellulose nanofiber composite substrates for flexible electronics. In: 2012 TAPPI international conference on nanotechnology for renewable materials, Montreal, QC

Saito T, Hirota M, Tamura N, Kimura S, Fukuzumi H, Heux L, Isogai A (2009) Individualization of nano-sized plant cellulose fibrils by direct surface carboxylation using TEMPO catalyst under neutral conditions. Biomacromecules 10(7):1992–1996

Segal L, Creely JJ, Martin AE Jr, Conrad CM (1962) An empirical method for estimating the degree of crystallinity

of native cellulose using the X-ray diffractometer. Text Res J 29(10):786–794

Sehaqui H, Liu A, Zhou Q, Berglund LA (2010) Fast preparation procedure for large, flat cellulose and cellulose/inorganic nanopaper structures. Biomacromolecules 11(9):2195–2198

Sehaqui H, Mushi NE, Morimune S, Salajkova M, Nishino T, Berglund LA (2012) Cellulose nanofiber orientation in nanopaper and nanocomposites by cold drawing. ACS Appl Mater Interfaces 4(2):1043–1049

Siró I, Plackett D (2010) Microfibrillated cellulose and new nanocomposites materials: a review. Cellulose 17(3):459–494

Spence KL, Venditti RA, Habibi Y, Rojas OJ, Pawlak JJ (2010) The effect of chemical composition on microfibrillar cellulose films from wood pulps: mechanical processing and physical properties. Bioresour Technol 101(15):5961–5968

Svagan AJ, Jensen P, Dvinskikh SV, Furó I, Berglund LA (2010) Towards tailored hierarchical structures in cellulose nanocomposite biofoams prepared by freezing/freeze-drying. J Mater Chem 20(32):6646–6654

Tonoli GHD, Teixeira EM, Corrêa AC, Marconcini JM, Caixeta LA, Pereira-da-Silva MA, Mattoso LHC (2012) Cellulose micro/nanofibers from eucalyptus kraft pulp: preparation and properties. Carbohyd Polym 89(1):80–88

Turbak A, Snyder FW, Sandberg KR (1983) Microfibrillated cellulose, a new cellulose product: properties, uses, and commercial potential. J Appl Polym Sci Appl Polym Symp 37(9):815–827

Uddin AJ, Araki J, Gotoh Y (2011) Toward "strong" green nanocomposites: polyvinyl alcohol reinforced with extremely oriented cellulose whiskers. Biomacromolecules 12(3):617–624

Xhanari K, Syverud K, Chinga-Carrasco G, Paso K, Stenius P (2011) Reduction of water wettability of nanofibrillated cellulose by adsorption of cationic surfactants. Cellulose 18(2):257–270